

## Switched adaptive control of air handling units with discrete and saturated actuators

Yuan, Shuai; Zhang, Lixian; Holub, Ondrej; Baldi, Simone

**DOI**

[10.1109/LCSYS.2018.2840041](https://doi.org/10.1109/LCSYS.2018.2840041)

**Publication date**

2018

**Document Version**

Accepted author manuscript

**Published in**

IEEE Control Systems Letters

**Citation (APA)**

Yuan, S., Zhang, L., Holub, O., & Baldi, S. (2018). Switched adaptive control of air handling units with discrete and saturated actuators. *IEEE Control Systems Letters*, 2(3), 417-422.  
<https://doi.org/10.1109/LCSYS.2018.2840041>

**Important note**

To cite this publication, please use the final published version (if applicable).  
Please check the document version above.

**Copyright**

Other than for strictly personal use, it is not permitted to download, forward or distribute the text or part of it, without the consent of the author(s) and/or copyright holder(s), unless the work is under an open content license such as Creative Commons.

**Takedown policy**

Please contact us and provide details if you believe this document breaches copyrights.  
We will remove access to the work immediately and investigate your claim.

# Switched Adaptive Control of Air Handling Units With Discrete and Saturated Actuators

Shuai Yuan<sup>1</sup>, Lixian Zhang<sup>1</sup>, *Fellow, IEEE*, Ondrej Holub, and Simone Baldi<sup>2</sup>

**Abstract**—This letter introduces a new switched adaptive control mechanism that can cope with parametric uncertainty while using discrete and saturated actuators. Control of air handling units (AHUs), where air and water supply have discrete and saturated characteristics, is the motivational drive behind this letter. We show that the cheap actuation and low computational requirements of building automation installations can be met after recasting the AHU thermal dynamics as a switched linear system with discrete working modes. Adaptive laws with anti-windup compensation and a switching law based on dwell time are introduced to cope with the uncertainties and input constraints of the switched linear system. Tracking performance is shown analytically and demonstrated via a numerical test case.

**Index Terms**—Air handling units, switched adaptive control, input saturation, discrete input, dwell time.

## I. INTRODUCTION

AT THE core of heating, ventilating and air-conditioning (HVAC) systems in modern buildings are air handling units (AHUs), whose task is to provide air at desired temperature and humidity [1]–[3]. Considerable efforts have been made to provide efficient control for AHUs, where at least two intrinsic features of AHUs stand out [4]: first, the interaction between the air circuit and the water circuit in the heating/cooling coil gives rise to *nonlinear dynamics*; second, custom installation settings and variable operating conditions induce substantial *uncertainty* and several undetermined operating parameters. As a way to address nonlinearities and uncertainties, intelligent control techniques,

such as fuzzy logic and/or genetic algorithm have been proposed for AHUs [5], [6]. Genetic-based optimal control was adopted in [7] and [8] to maintain the temperature set point. In [9], model predictive HVAC control was adopted to minimize energy cost while guaranteeing comfort.

Unfortunately, the effectiveness of these approaches is usually put at stake when considering two fundamental limitations of building automation: computational complexity and cheap actuation devices. To provide flexible products with the widest market, it is often desirable to embed the building automation intelligence in cheap hardware with moderate computational capabilities. However, model predictive controllers require high-performance hardware, while the design of good fuzzy/genetic rules is typically tailored to a specific installation and difficult to be mass-produced [10]. For similar mass production motivations, mechanical actuation parts in building automation systems are designed to be simple, cheap and robust [11]. This means that variable speed drives/valves will not be capable of the very accurate control adjustments required by predictive or fuzzy methods, but they will usually work at a discrete set of speeds/positions [12]. In view of the practical configurations of AHUs, delivering an intelligent control that can cope with these limitations is both a significant challenge and a key opportunity for the building automation industry [13], [14], which motivates this letter.

In this letter, a novel switched adaptive control method is proposed to cope with uncertainties and nonlinearities of AHUs with discrete and saturated inputs. First, a switched AHU model is established by linearizing the nonlinear dynamics with respect to discrete working modes, i.e., different fan speeds. A family of reference models is used to represent the desired system dynamics for each working mode. An adaptive law with anti-windup compensator and a switching law based on dwell time are designed to deal with uncertainties of the switched system, and with the saturated and quantized valve characteristics. The main contribution of this letter is twofold: 1) the complex nonlinear model of AHU is recast into a switched linear system, which simplifies the controller design and reduces computational complexity; 2) a novel adaptive control strategy is developed, which specifically addresses practical input constraints in AHUs.

This letter is organized as follows: Section II introduces the model of AHU and the control problem. The switched adaptive control scheme is given in Section III. A case study is presented in Section IV to illustrate the proposed method and this letter is concluded in Section V.

Manuscript received March 6, 2018; revised April 26, 2018; accepted May 10, 2018. Date of publication May 23, 2018; date of current version June 11, 2018. This work was supported by the Marie-Curie Action (Advanced Methods for Building Diagnostics and Maintenance) under Grant FP7-PEOPLE-451 2012-IAPP. Recommended by Senior Editor M. Guay. (*Corresponding author: Shuai Yuan.*)

S. Yuan is with the School of Astronautics, Harbin Institute of Technology, Harbin 150080, China, and also with the Delft Center for Systems and Control, Delft University of Technology, 2628 Delft, The Netherlands (e-mail: xiaoshuaihust@hotmail.com).

L. Zhang is with the School of Astronautics, Harbin Institute of Technology, Harbin 150080, China (e-mail: lixianzhang@hit.edu.cn).

O. Holub is with the Honeywell Prague Laboratory, Building Automation Department, 148 00 Prague, Czech Republic (e-mail: ondrej.holub@honeywell.com).

S. Baldi is with the Delft Center for Systems and Control, Delft University of Technology, 2628 Delft, The Netherlands (e-mail: s.baldi@tudelft.nl).

Digital Object Identifier 10.1109/LCSYS.2018.2840041

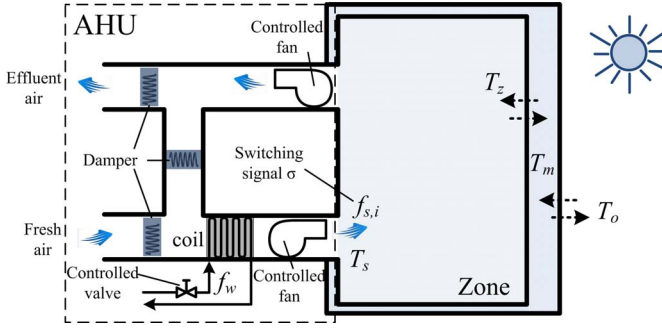


Fig. 1. Layout of the AHU with a single zone.

*Notation.* The notation used in this letter is as follows: we define  $\mathbf{He}\{P\} = P^T + P$ , where the superscript  $T$  represents the transpose. The notation  $\|\cdot\|$  represents the Euclidean norm of a vector. The operators  $\lambda_{\max}(P)$  and  $\lambda_{\min}(P)$  return the maximum and minimum eigenvalues of the square matrix  $P$ , respectively. The operator  $\text{sgn}$  extracts the sign of a real number.

## II. PROBLEM FORMULATION AND PRELIMINARIES

We consider an air handling unit serving a conditioned space. Such space is taken as a single zone, for the sake of simplicity. The air handler consists of a cooling/heating coil, supply and return fans, valve, damper, and ductwork, as shown in Fig. 1. Depending on different seasons, chilled or heated water flows through the coil, so that the air in the ductwork is cooled or heated in its path. The water flow rate is controlled by the position of a programmable valve, while the air flow rate is controlled by the speed of the supply/return fan. In this letter we focus on a heating coil case. The temperature in the zone is also affected by the heat exchange with the building mass, and by the solar radiation.

All these effects can be described using the heat balance of the zone. In particular, after ignoring the influence of humidity on temperature (in line with [5] and [6]), the following differential equations describe the evolution of temperature in the system:

$$\begin{aligned} \dot{T}_z &= -\frac{f_{s,i}}{V_z}(T_z - T_s) + \frac{k_{mz}}{\rho_a C_{pa} V_z}(T_m - T_z) + \frac{\eta P_{\text{solar}}}{\rho_a C_{pa} V_z} \\ \dot{T}_m &= \frac{k_{mz}}{C_m}(T_z - T_m) + \frac{k_{om}}{C_m}(T_o - T_m) + \frac{1 - \eta}{C_m} P_{\text{solar}} \\ \dot{T}_s &= \frac{f_{s,i}}{V_c}(T_z - T_s) + \frac{0.25 f_{s,i}}{V_c}(T_o - T_z) + \frac{\rho_w C_{pw} \Delta T_c}{\rho_a C_{pa} V_c} f_w \end{aligned} \quad (1)$$

where the definitions of all parameters in (1) are given in Table I. The following comments apply to  $T_m$ ,  $f_{s,i}$  and  $f_w$  in (1). Even if the temperature  $T_m$  of the building mass represents the agglomeration of many thermal capacities, methods have been developed estimate it with some accuracy (see [2]): therefore, such an estimate can be employed for feedback. In most building automation designs, the variable-speed drive of the fan operates at fixed number of speeds [12], typically  $\{\text{off}, \text{low}, \text{medium}, \text{high}\} = \{0, 1, 2, 3\}$ , giving  $f_{s,i} \in \{f_{s,0}, f_{s,1}, f_{s,2}, f_{s,3}\}$  with  $f_{s,0} \equiv 0$ . The switching behavior between different fan speeds, i.e.,  $f_{s,i} = f_{s,\sigma(t)}$ , is controlled by a switching signal  $\sigma(\cdot)$ , which might depend on external commands or on a supervisory controller. The presence of switching phenomena requires us to give the following

TABLE I  
PARAMETERS OF THE DYNAMICAL MODEL OF THE AHU

$C_{pa}$ (J/kg $^\circ$ C)	Specific heat capacity of air
$C_{pw}$ (J/kg $^\circ$ C)	Specific heat capacity of water
$C_m$ (J/ $^\circ$ C)	Heat capacity of the mass
$k_{om}$ (W/ $^\circ$ C)	Thermal conductance between environmental air and the mass
$k_{mz}$ (W/ $^\circ$ C)	Thermal conductance between indoor air and the mass
$\rho_a$ (kg/m $^3$ )	Air density
$\rho_w$ (kg/m $^3$ )	Water density
$V_c$ (m $^3$ )	Volume of heat exchanger
$V_z$ (m $^3$ )	Volume of thermal space
$T_o$ ( $^\circ$ C)	Environmental temperature
$T_s$ ( $^\circ$ C)	Temperature of supply air
$T_z$ ( $^\circ$ C)	Temperature of thermal zone
$T_m$ ( $^\circ$ C)	Temperature of mass in the zone
$f_s$ (m $^3$ /s)	Flow rate of air with discrete modes
$f_w$ (m $^3$ /s)	Flow rate of chilled water
$\Delta T_c$ ( $^\circ$ C)	Temperature gradient in cooling unit
$P_{\text{solar}}$ (kW/m $^2$ )	Solar radiation
$\eta$	Percentage of direct solar radiation

specifications on how often dynamics can switch (switching law design).

*Definition 1 (Dwell Time Switching) [15]:* Switching laws with switching sequence  $S := \{t_l\}_{l \in \mathbb{N}^+}$  are said to be *dwell-time admissible* if there exists a number  $\tau_d > 0$  such that  $t_{l+1} - t_l \geq \tau_d$  holds for all  $l \in \mathbb{N}^+$ . Any positive number  $\tau_d$  for which this constraint holds is called *dwell time*, and the set of dwell time admissible switching laws is denoted by  $D(\tau_d)$ .

*Remark 1:* Definition 1 formalizes the fact that the fan speed cannot change arbitrarily fast. Therefore, in case user violates the dwell time constraint by changing the speed too often, a controller will supervise the switching transitions.

As far as  $f_w$  is concerned, in many building automation designs, valves are adjusted to discrete positions within a bounded range. In other words, the water flow rate turns out to be discretized and saturated as described by

$$\text{sat}(q(f_w)) = \begin{cases} \text{sgn}(q(f_w)) f_{\max}, & |f_w| \geq f_{\max} \\ q(f_w), & |f_w| < f_{\max} \end{cases} \quad (2)$$

where  $f_{\max}$  is the maximum flow rate of heated water and  $q(f_w)$  represents the discretized valve of  $f_w$ , which satisfies

$$|q(f_w) - f_w| \leq \Delta_{\max} \quad (3)$$

where  $\Delta_{\max}$  is an upper bound of the discrete error.

By taking into account the switching behavior of  $f_{s,i}$  and the practical constraints of  $f_w$ , and by selecting the state  $x = [T_z \ T_m \ T_s]^T$ , the model (1) is recast into in a switched input-saturated system with four different modes (subsystems)

$$\dot{x}(t) = A_i x(t) + b \text{sat}(q(f_w(t))) + d(t) \quad (4)$$

for  $i \in \{0, 1, 2, 3\}$ , where

$$A_i = \begin{bmatrix} -\alpha_1 f_{s,i} - \alpha_2 k_{mz} & -\alpha_2 k_{mz} & \alpha_1 f_{s,i} \\ \beta_1 k_{mz} & -\beta_1 (k_{mz} + k_{om}) & 0 \\ 0.75 \beta_2 f_{s,i} & 0 & -\beta_2 f_{s,i} \end{bmatrix}$$

$$b = [0 \ 0 \ \gamma_1]^T, \quad d = d_1 + d_2$$

with  $d_1 = [0 \ 0 \ \gamma_2]^T f_{s,i}$ ,  $d_2 = [\xi_1 \ \xi_2 \ 0]^T$

$$\alpha_1 = \frac{1}{V_z}, \quad \alpha_2 = \frac{1}{\rho_a C_{pa} V_z}, \quad \beta_1 = \frac{1}{C_m}, \quad \beta_2 = \frac{1}{V_c}$$

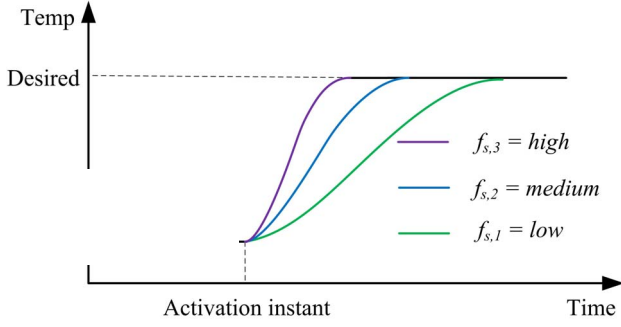


Fig. 2. The desired dynamics of the temperature of the zone.

$$\gamma_1 = \frac{\rho_w C_{pw} \Delta T_c}{\rho_a C_{pa} V_c}, \quad \gamma_2 = 0.25 \beta_2 T_o, \quad \xi_1 = \frac{\eta}{\rho_a C_{pa} V_z} P_{solar}$$

$$\xi_2 = (1 - \eta) P_{solar} / C_m + \beta_1 k_{om} T_o.$$

Since normally a minimum ventilation rate must be guaranteed according to the *ASHRAE Standard 62-1989* [16], we will focus on control of subsystems  $i \in M$ , where  $M$  denotes the set  $\{1, 2, 3\}$ . Noticing that the values of the volume of heat exchanger  $V_c$  and of the temperature gradient in the heating unit  $\Delta T_c$  are installation-dependent and *a priori* unspecified, the parameters  $\beta_2$  and  $\gamma_1$  in (4) are unknown. This introduces large parametric uncertainties that make the control of the switched input-saturated systems (4) an open problem.

*Remark 2:* Instead of considering the “ideal” nonlinear model (1) as in [17] and [18], model (4) captures the “realistic” AHU configuration in which the fan and the valve operate in a discrete number of modes, and thus cannot be adjusted continuously. To the best of the authors’ knowledge, no AHU control method has been provided in literature for system (4), which thus requires a new control scheme.

To deal with the uncertainties in (4), techniques from model reference adaptive control are adopted. We design three reference models for subsystems 1, 2, 3 in the following form:

$$\dot{x}_m(t) = A_{m,i} x_m(t) + b_{m,i} T_d, \quad i \in M \quad (5)$$

with

$$A_{m,i} = \begin{bmatrix} -\alpha_1 f_{s,i} - \alpha_2 k_{mz} & -\alpha_2 k_{mz} & \alpha_1 f_{s,i} \\ \beta_1 k_{mz} & -\beta_1 (k_{mz} + k_{om}) & 0 \\ \delta_{m1,i} & \delta_{m2,i} & -\delta_{m3,i} \end{bmatrix}$$

$$b_{m,i} = [0 \quad 0 \quad \delta_{m4,i}]^T$$

where  $x_m$  is the desired dynamics of the uncertain switched system (4),  $T_d$  represents the desired temperature set point, and the positive scalars  $\delta_{mk,i}$ ,  $k = 1, 2, 3, 4$ , are parameters to be designed as in the following remark.

*Remark 3:* The discrete fan speeds  $\{f_{s,1}, f_{s,2}, f_{s,3}\}$  lead to a straightforward design for (5). In particular, the dynamics of the reference model are designed to be fast or slow according to the fan speed: the higher the speed, the faster the rate with which the temperature is expected to change, see Fig. 2.

Since we are interested in an adaptation transient in the order of minutes, we can regard the outside temperature  $T_o$  and the solar radiation  $P_{solar}$  in (4) as constants during the adaptation process. Therefore, a nominal state feedback controller is designed as  $f_w(t) = k_i^{*T} x(t) + l_i^* T_d - v^*$ ,  $i \in M$ , where the nominal parameters  $k_i^* = [\kappa_{1,i}^*, \kappa_{2,i}^*, \kappa_{3,i}^*]^T$ ,  $l_i^*$ ,  $v^* \in \mathbb{R}$ , satisfy

the following matching conditions:

$$b_i k_i^{*T} = A_{m,i} - A_i, \quad b l_i^* = b_{m,i}, \quad b v^* = d_1. \quad (6)$$

The matching conditions (6) hold in view of the structure of the matrices in (4)–(5). However, without the knowledge of the parameters  $A_i$ ,  $b$ , and  $d_1$ , we cannot solve (6) and obtain the nominal parameters of the controller. Therefore, we adopt the controller

$$f_w(t) = k_i^T(t) x(t) + l_i(t) T_d - v(t) \quad (7)$$

where  $k_i(t)$ ,  $l_i(t)$ , and  $v(t)$  are the estimates of the nominal parameters  $k_i^*$ ,  $l_i^*$ ,  $v^*$ . The closed-loop system with controller (7) is rewritten as

$$\dot{x}(t) = A_i x(t) + b(k_i^T(t) x(t) + l_i(t) T_d - v(t)) - b(\Delta f_w + \Delta f) + d(t) \quad (8)$$

with  $\Delta f_w = q(f_w) - \text{sat}(q(f_w))$  and  $\Delta f = f_w - q(f_w)$ . Define the tracking error  $e = x - x_m$ . Using the matching conditions (6) and subtracting (5) from (8) give us

$$\dot{e}(t) = A_{m,i} e(t) + b(\tilde{k}_i^T(t) x(t) + \tilde{l}_i(t) T_d - \tilde{v}(t)) - b(\Delta f_w + \Delta f) + d_2(t) \quad (9)$$

with the parameter estimation errors being  $\tilde{k}_i(t) = k_i(t) - k_i^*$ ,  $\tilde{l}_i(t) = l_i(t) - l_i^*$ ,  $\tilde{v}(t) = v(t) - v^*$ . Therefore, the control objective of this letter is stated as:

*Problem 1:* Design a switched adaptive control method, consisting of an adaptive law and of a dwell time switching law for (7), which guarantees that the switched system (4) with saturated and discrete input can track the reference model (5) with bounded tracking error  $e$  in (9).

### III. SWITCHED ADAPTIVE CONTROL

The switched adaptive control framework used to solve Problem 1 is explained in Fig. 3, consisting of three key elements: a family of reference models representing the desired behavior of the zone temperature; an adaptive mechanism to update the controller; a switching signal  $\sigma(\cdot)$ . Before introducing the adaptive laws, the following lemma is recalled.

*Lemma 1* [19]: Given an integer  $K$  and a time interval  $h > 0$ , if there exists a collection of symmetric matrices  $P_{i,k} > 0$ ,  $i \in M$ ,  $k = 0, \dots, K$ , such that the following conditions hold:

$$(P_{i,k+1} - P_{i,k})/h + P_{i,k} A_{m,i} + A_{m,i}^T P_{i,k} < 0$$

$$\text{for } K = k, k + 1; k = 0, \dots, K - 1 \quad (10a)$$

$$P_{i,K} A_{m,i} + A_{m,i}^T P_{i,K} < 0 \quad (10b)$$

$$P_{i,K} - P_{j,0} \geq 0 \quad (10c)$$

for  $j, i \in M$  with  $j \neq i$ , then the switched system  $\dot{x} = A_{m,i} x$  is asymptotically stable for any switching signal  $\sigma(\cdot) \in D(\tau_d)$  with  $\tau_d = Kh$ .

To eliminate the windup effect possibly caused by the saturation constraint (2), the following anti-windup compensator inspired by [20] is used for developing the adaptive law:

$$\dot{x}_{aw}(t) = A_{m,i} x_{aw}(t) - b_{aw,i}(t) \Delta f_w(t) \quad (11)$$

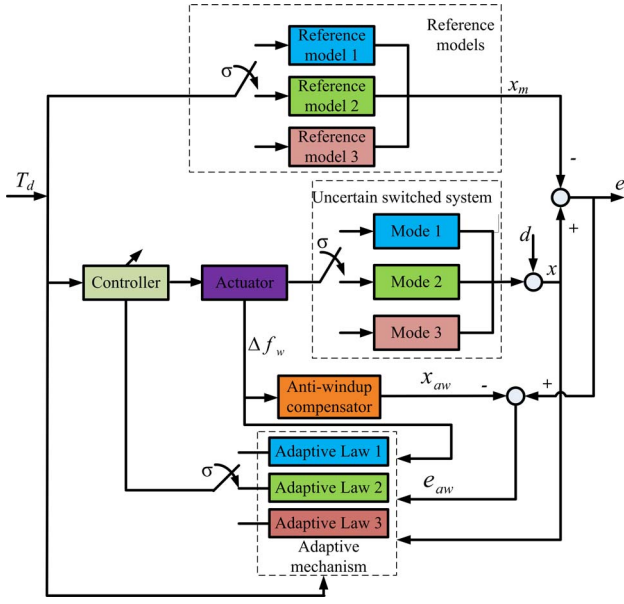


Fig. 3. Switched adaptive control scheme.

with  $x_{aw}(t_0) = 0$ , where  $b_{aw,i}(t) \in \mathbb{R}^3$  is a parameter to be estimated. A new error is defined as  $e_{aw} = e - x_{aw}$ , whose dynamics are

$$\begin{aligned} \dot{e}_{aw} = & A_{m,i}e_{aw} + b \left( \tilde{k}_i^T(t)x(t) + \tilde{l}_i(t)T_d - \tilde{v}(t) \right) \\ & - \tilde{b}_{aw,i}\Delta f_w(t) - b\Delta f + d_2(t) \end{aligned} \quad (12)$$

where  $\tilde{b}_{aw,i}(t) = b - b_{aw,i}(t)$ . In order to obtain a well-posed bound on the tracking error, one conventional assumption [21], [22] is necessary for the adaptive law.

*Assumption 1:* The parameters  $k_i^*$ ,  $l_i^*$ ,  $v^*$ , and  $b$  are confined within known bounds, i.e.,  $k_i^* \in [\underline{k}_i, \bar{k}_i]$ ,  $l_i^* \in [\underline{l}_i, \bar{l}_i]$ ,  $v^* \in [\underline{v}, \bar{v}]$ , and  $b \in [\underline{b}, \bar{b}]$ . In addition, let  $\bar{d}_2$  be the upper bound of  $\|d_2\|$ .

Therefore, according to the anti-windup scheme (11)–(12), to Lemma 1 and to Assumption 1, the following adaptive laws for  $k_i$ ,  $l_i$ ,  $v$ , and  $b_{aw,i}$  are proposed:

$$\begin{aligned} \dot{k}_i(t) &= -\Gamma_i x(t) e_{aw}^T(t) P_i(t) b_{mi} + f_{k,i}(t) \\ \dot{l}_i(t) &= -\gamma_{l,i} r(t) e_{aw}^T(t) P_i(t) b_{mi} + f_{l,i}(t) \\ \dot{v}(t) &= \gamma_{v,i} e_{aw}^T(t) P_i(t) b_{mi} + f_{v,i}(t) \\ \dot{b}_{aw,i}^T(t) &= \gamma_{b,i} \Delta f_w e_{aw}^T(t) P_i(t) + f_{b,i}(t) \end{aligned} \quad (13)$$

where  $\Gamma_i \in \mathbb{R}^{3 \times 3}$ ,  $\gamma_{l,i}$ ,  $\gamma_{v,i}$ , and  $\gamma_{b,i} \in \mathbb{R}$  are positive adaptive gains for  $i \in M$ , and the time-varying matrix  $P_i(t)$  arises from linear interpolation of  $P_{i,k}$  as follows:

$$P_i(t) = \begin{cases} P_{i,k} + \Delta P_{k,k+1}^i \rho_{\ell,k}(t), & t \in [t_{\ell,k}, t_{\ell,k+1}) \\ P_{i,K}, & t \in [t_{\ell,K}, t_{\ell+1}) \end{cases} \quad (14)$$

with  $\rho_{\ell,k}(t) = (t - t_{\ell,k})/h$  and  $\Delta P_{k,k+1}^i \triangleq P_{i,k+1} - P_{i,k}$ .

The terms  $f_{k,i}$ ,  $f_{l,i}$ ,  $f_{v,i}$ , and  $f_{b,i}$  in (13) are projection functions, as defined in [23] and [24], which guarantees that the estimates are within the bounds of Assumption 1. The following main result holds.

*Theorem 1:* Consider the switched uncertain model of the AHU (4) with saturated and discontinuous input. Then, using the controller (7), the anti-windup compensator (11), and the adaptive laws (13)–(14), all signals of the closed-loop

system are bounded, and the norm of the tracking error  $\|e\|$  is of the order of  $\mathcal{O}(B + \sup(\Delta f_w))$  for any switching signal  $\sigma(\cdot) \in D(\tau_d)$ , where

$$B = \frac{2 \max_{i \in M} \lambda_{\max}(P_i) (\|\bar{d}_2\| + \Delta_{\max} b)}{\min_{i \in M} \lambda_{\min}(A_{m,i}^T P_i + P_i A_{m,i} + \dot{P}_i)}.$$

*Proof:* Consider the following Lyapunov function

$$\begin{aligned} V(t) = & e_{aw}^T(t) P_{\sigma(t)}(t) e_{aw}(t) + \sum_{\ell=1}^3 \frac{1}{|l_\ell^*|} \tilde{k}_\ell^T \Gamma_\ell^{-1} \tilde{k}_\ell \\ & + \sum_{\ell=1}^3 \frac{\gamma_{l,\ell}^{-1}}{|l_\ell^*|} \tilde{l}_\ell^2 + \frac{\gamma_{v,\sigma(t)}^{-1}}{|l_\ell^*|} \tilde{v}^2 + \sum_{\ell=1}^3 \frac{\gamma_{b,\ell}^{-1}}{|l_\ell^*|} \tilde{b}_{aw,\ell}^2. \end{aligned} \quad (15)$$

Without loss of generality, assume that subsystem  $i$  is active for  $t \in [t_\ell, t_{\ell+1})$  and subsystem  $j$  is active for  $t \in [t_{\ell+1}, t_{\ell+2})$ . For  $t \in [t_{\ell,k}, t_{\ell,k+1})$ , the time derivative of  $V$  is

$$\begin{aligned} \dot{V} = & e_{aw}^T Q_i e_{aw} + e_{aw}^T P_i d_2 + d_2^T P_i e_{aw} + e_{aw}^T \Delta_f P_i b \\ & + b^T \Delta_f P_i e_{aw} + \frac{1}{|l_i^*|} \tilde{k}_i^T \Gamma_i^{-1} f_{k,i} + \frac{1}{|l_i^*|} \tilde{l}_i^T \gamma_{l,i}^{-1} f_{l,i} \\ & + \frac{1}{|l_i^*|} \tilde{v} \gamma_{v,i}^{-1} f_{v,i} + \frac{1}{|l_i^*|} \tilde{b}_{aw,i} \gamma_{b,i}^{-1} f_{b,i} \end{aligned} \quad (16)$$

with  $Q_i = A_{m,i}^T P_i + P_i A_{m,i} + \dot{P}_i$ . To study the properties of  $V(t)$  for  $t \in [t_\ell, t_{\ell+1})$ , first we consider a sub-interval, i.e.,  $t \in [t_{\ell,k}, t_{\ell,k+1})$ ,  $k = 0, \dots, K-1$ . Note that

$$\begin{aligned} Q_i(t) = & \mathbf{He}\{P_i(t) A_{m,i}\} + \Delta P_{k+1,k}^i / h \\ & + (\omega_1 P_{i,k} + \omega_2 P_{i,k+1}) \\ = & \omega_1 [\Delta P_{k+1,k}^i / h + \mathbf{He}\{P_{i,k} A_{m,i}\}] \\ & + \omega_2 [\Delta P_{k+1,k}^i / h + \mathbf{He}\{P_{i,k+1} A_{m,i}\}] \end{aligned} \quad (17)$$

where  $\omega_1 = 1 - (t - t_{\ell,k})/h$ , and  $\omega_2 = 1 - \omega_1$ . According to (10a), it follows that

$$Q_i(t) < 0, \quad t \in [t_{\ell,k}, t_{\ell,k+1}). \quad (18)$$

Then, let us consider  $t \in [t_{\ell,K}, t_{\ell+1})$  for the case that  $t_{\ell+1} - t_\ell > \tau_d$ . We have  $P_i(t) = P_{i,K}$  according to (14), which indicates by (10b) that

$$Q_i(t) < 0, \quad t \in [t_{\ell,K}, t_{\ell+1}). \quad (19)$$

Since the signals  $e_{aw}(\cdot)$ ,  $\tilde{k}_{\sigma(\cdot)}(\cdot)$ ,  $\tilde{l}_{\sigma(\cdot)}(\cdot)$ , and  $\tilde{v}_{\sigma(\cdot)}(\cdot)$  are continuous according to (9) and (13), we have, at the switching instant  $t_{\ell+1}$ ,  $V_j(t_{\ell+1}) - V_i(t_{\ell+1}^-) = e_{aw}^T(t_{\ell+1})(P_{j,0} - P_{i,K})e_{aw}(t_{\ell+1})$ , which indicates that  $V(\cdot)$  is non-increasing at switching instant  $t_{\ell+1}$  considering  $P_{i,0} - P_{j,K} \leq 0$  for  $i, j \in M$  in (10c). According to the definition of parameter projection, it follows  $\tilde{k}_i^T \Gamma_i^{-1} f_{k,i} \leq 0$ ,  $\tilde{l}_i^T \gamma_{l,i}^{-1} f_{l,i} \leq 0$ ,  $\tilde{v} \gamma_{v,i}^{-1} f_{v,i} \leq 0$ , and  $\tilde{b}_{aw,i} \gamma_{b,i}^{-1} f_{b,i} \leq 0$ . Then, together with (3), (18)–(19), we have  $\dot{V} \leq -\lambda_{\min}(Q_i) \|e_{aw}\|^2 + 2\lambda_{\max}(P_i) (\|\bar{d}_2\| + \Delta_{\max} b) \|e_{aw}\|$ , which implies that for  $\|e_{aw}\| \geq B$ , we have  $\dot{V} < 0$ . In other words, the error  $e_{aw}(\cdot)$  is attracted into the ball centered in the origin with radius  $B$ . Since the matrix  $A_i$  of the temperature dynamic model (4),  $i \in M$ , is stable,  $x(t)$  is bounded for any  $t \geq t_0$ . Note that the parameter estimates are bounded by the projection laws. According to (7) and (11), this will lead to the boundedness of  $\Delta f_w$  and  $x_{aw}$ . Recalling  $e = e_{aw} + x_{aw}$ , we can

obtain that the norm of the tracking error  $\|e\|$  is of the order of  $\mathcal{O}(\mathcal{B} + \sup(\Delta f_w))$ . This completes the proof. ■

As compared to [19], this letter shows that multiple Lyapunov functions that are non-increasing at switching instants can be obtained even in the presence discrete and saturated input. Note that as the adaptive laws (13) employ parameter projection, it is well-known from robust adaptive literature of [21, Ch. 8] that stability of the closed-loop is preserved even in the presence of some model errors and external disturbance.

#### IV. CASE STUDY

Let us consider a single zone as in Fig. 1 in line with [6]. The material of the building mass is burnt brick, whose density is  $1820\text{kg/m}^3$ , specific heat is  $880\text{J/kg}^\circ\text{C}$ , the thermal exchange coefficient between the environmental air and the mass  $k_{om}/C_m = 9.72 \cdot 10^{-6}\text{1/s}$ , between the indoor air and mass  $k_{mz}/C_m = 5.235 \cdot 10^{-5}\text{1/s}$  [2], and absorptivity of the solar radiation is 0.6. The discretization error of the water supply rate is  $0.05\text{L/s}$  and the water supply rate is constrained in  $[0\ 2.5]\text{L/s}$ . The desired zone temperature is  $24^\circ\text{C}$ , and the initial zone temperature is  $16^\circ\text{C}$ .

##### A. Design of Reference Models

The following reference models for three different fan speeds are designed:

$$A_{m,1} = \begin{bmatrix} -0.0066 & -0.0001 & 0.0065 \\ 0.0002 & -0.0003 & 0 \\ 3.2 & 0 & -4.4 \end{bmatrix}, \quad b_{m,1} = \begin{bmatrix} 0 \\ 0 \\ 1.2638 \end{bmatrix}$$

$$A_{m,2} = \begin{bmatrix} -0.0126 & -0.0001 & 0.0125 \\ 0.0002 & -0.0003 & 0 \\ 3 & 0 & -4.1 \end{bmatrix}, \quad b_{m,2} = \begin{bmatrix} 0 \\ 0 \\ 1.1310 \end{bmatrix}$$

$$A_{m,3} = \begin{bmatrix} -0.0201 & -0.0001 & 0.02 \\ 0.0002 & -0.0003 & 0 \\ 2.5 & 0 & -3.6 \end{bmatrix}, \quad b_{m,3} = \begin{bmatrix} 0 \\ 0 \\ 1.1169 \end{bmatrix}.$$

Solving the LMIs (10a)–(10c) for  $K = 1$  using SeDuMi solver [25], we obtain the dwell time  $\tau_d = 1.2\text{s}$ . Let the initial conditions be  $x(0) = [16\ 5\ 16]^T$ ,  $x_m(0) = [16.5\ 5\ 16.5]^T$ ,  $k_1(0) = [0.2941\ 0\ -0.4234]^T \times 10^{-4}$ ,  $k_2(0) = [-0.1764\ 0\ 0.2117]^T \times 10^{-4}$ ,  $k_3(0) = [-0.823\ 0\ 1.035]^T \times 10^{-4}$ ,  $l_1(0) = 2.9731 \times 10^{-5}$ ,  $l_2(0) = 2.6606 \times 10^{-5}$ ,  $l_3(0) = 2.6606 \times 10^{-5}$ ,  $v(0) = 4.7049 \times 10^{-8}$ ,  $b_{aw,i}(0) = [0\ 0\ 1.0627]^T \times 10^4$  for  $i \in M$ . Since the dwell time  $\tau_d = 1.2\text{s}$  is negligible as compared to the actual operational time of the fan, very fast switching is allowed with guaranteed stability of the switched linear system (4). Hence, two switching strategies, time-driven and temperature-dependent, will be designed in the following. To show the robustness of the adaptive laws (13), we consider some modeling errors consisting of unmodelled system matrices  $\Delta A_i = 0.1A_i$  and  $\Delta b = 0.1b$  for  $i = 1, 2, 3$ , as well as a disturbance introduced by some occupants in the zone where each occupant generates additional  $200\text{W}$  of heat gain [26].

##### B. Scenario I: Time-Driven Switching

We assume that the mode of the fan is switched to meet the regulations for air exchange needed for acceptable CO2

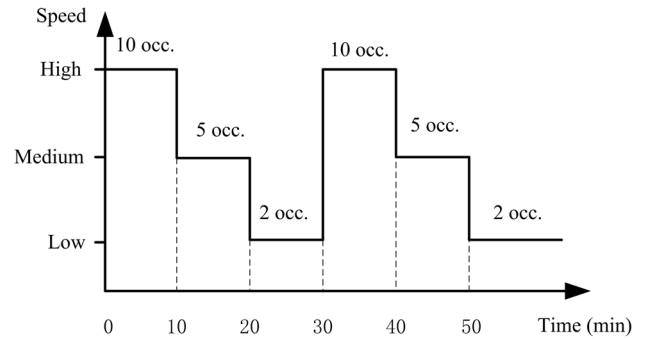


Fig. 4. The time-driven switching signal.

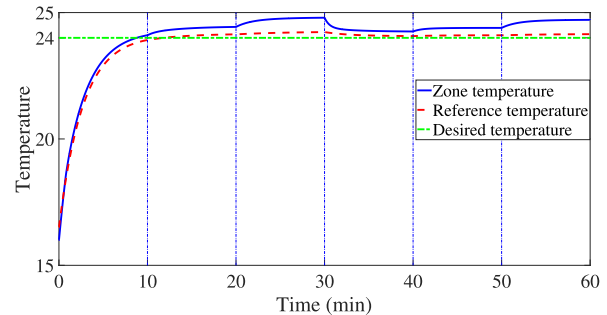


Fig. 5. The dynamics of the zone temperature under switching law Fig. 4.

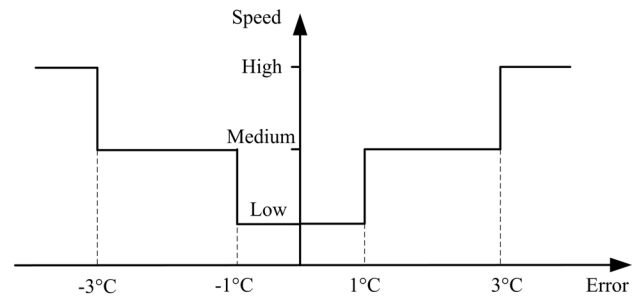


Fig. 6. The temperature-dependent switching signal.

levels: the larger the occupancy (and thus CO2 concentration), the higher the fan speed, as shown in Fig. 4. We consider that the size of occupancy changes every 10 minutes in 60 minutes.

The corresponding evolution of the zone temperature and of the reference zone temperature are shown in Fig. 5. The tracking error is bounded despite the presence of unmodeled dynamics and disturbances, which shows that the proposed adaptive laws (13) are robust.

##### C. Scenario II: Temperature-Dependent Switching

In this scenario, the switching mechanism is designed based on the rules shown in Fig. 6: when the difference between the zone temperature and the set point is bigger than  $3^\circ\text{C}$ , the fan operates at high speed; when the difference is in the interval  $[1\ 3]^\circ\text{C}$ , the fan operates at medium speed; when the difference is less than  $0.5^\circ\text{C}$ , the fan operates at low speed. The corresponding evolution of the zone temperature and of the reference zone temperature are depicted in Fig. 7, which shows a satisfactory tracking performance.

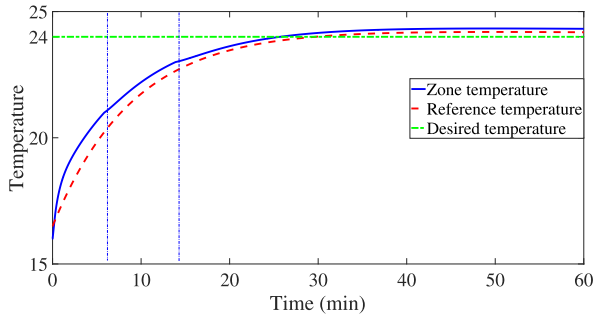


Fig. 7. The dynamics of the zone temperature under switching law Fig. 6.

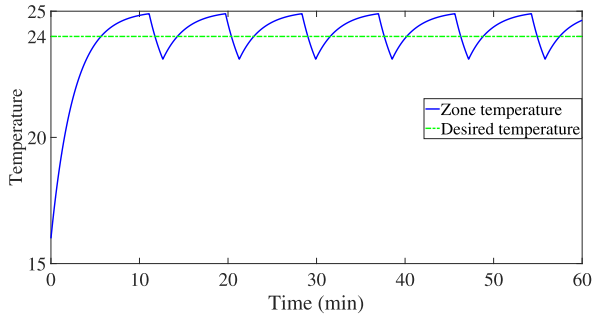


Fig. 8. The dynamics of the zone temperature with deadband on-off controller.

#### D. Deadband On-Off Control

A comparison with a conventional deadband on-off control method [27] is considered where maximum (ON) or zero (OFF) water flow rate is selected based on a temperature deadband. As compared to Fig. 5 and Fig. 7, Fig. 8 shows that, to achieve a comparable accuracy as the proposed method, a small deadband is needed, which leads to undesirable fast oscillations of the zone temperature and thus increases the maintenance burden of the fan.

### V. CONCLUSION

A switched adaptive control mechanism for air handling units has been developed to cope with system uncertainties and saturated and discontinuous input. The idealized nonlinear and uncertain air handling unit dynamics have been recast as a switched linear system with discrete air/water supply settings. By solving LMIs, an adaptive law with anti-windup compensation and a switching law based on dwell time have been introduced to cope with the uncertainties and input constraints of the switched linear system. Stability of the closed-loop system and tracking performance have been shown.

### REFERENCES

- [1] I. T. Michailidis, C. Korkas, E. B. Kosmatopoulos, and E. Nassie, "Automated control calibration exploiting exogenous environment energy: An Israeli commercial building case study," *Energy Build.*, vol. 128, pp. 473–483, Sep. 2016.
- [2] S. Baldi, S. Yuan, P. Endel, and O. Holub, "Dual estimation: Constructing building energy models from data sampled at low rate," *Appl. Energy*, vol. 163, pp. 81–92, May 2016.
- [3] M. Manic, D. Wijayasekara, K. Amarasinghe, and J. J. Rodriguez-Andina, "Building energy management systems: The age of intelligent and adaptive buildings," *IEEE Ind. Electron. Mag.*, vol. 10, no. 1, pp. 25–39, Mar. 2016.
- [4] C. Guo, Q. Song, and W. Cai, "A neural network assisted cascade control system for air handling unit," *IEEE Trans. Ind. Electron.*, vol. 54, no. 1, pp. 620–628, Feb. 2007.
- [5] M. W. Khan, M. A. Choudhry, M. Zeeshan, and A. Ali, "Adaptive fuzzy multivariable controller design based on genetic algorithm for an air handling unit," *Energy*, vol. 81, pp. 477–488, Mar. 2015.
- [6] H. Setayesh, H. Moradi, and A. Alasty, "A comparison between the minimum-order & full-order observers in robust control of the air handling units in the presence of uncertainty," *Energy Build.*, vol. 91, pp. 115–130, Mar. 2015.
- [7] S. Wang and X. Jin, "Model-based optimal control of VAV air-conditioning system using genetic algorithm," *Build. Environ.*, vol. 35, no. 6, pp. 471–487, 2000.
- [8] M. Mossolly, K. Ghali, and N. Ghaddar, "Optimal control strategy for a multi-zone air conditioning system using a genetic algorithm," *Energy*, vol. 34, no. 1, pp. 58–66, 2009.
- [9] J. D. Álvarez *et al.*, "Optimizing building comfort temperature regulation via model predictive control," *Energy Build.*, vol. 57, pp. 361–372, Feb. 2013.
- [10] H. Dibowski, J. Ploennigs, and K. Kabitzsch, "Automated design of building automation systems," *IEEE Trans. Ind. Electron.*, vol. 57, no. 11, pp. 3606–3613, Nov. 2010.
- [11] J. Khazaii, *Energy-Efficient HVAC Design: An Essential Guide for Sustainable Building*. Cham, Switzerland: Springer, 2014.
- [12] O. Holub, M. Zamani, and A. Abate, "Efficient HVAC controls: A symbolic approach," in *Proc. Eur. Control Conf. (ECC)*, Aalborg, Denmark, 2016, pp. 1159–1164.
- [13] E. Atam, "New paths toward energy-efficient buildings: A multispect discussion of advanced model-based control," *IEEE Ind. Electron. Mag.*, vol. 10, no. 4, pp. 50–66, Dec. 2016.
- [14] N. Cauchi, K. Macek, and A. Abate, "Model-based predictive maintenance in building automation systems with user discomfort," *Energy*, vol. 138, pp. 306–315, Nov. 2017.
- [15] W. Xiang and J. Xiao, "Stabilization of switched continuous-time systems with all modes unstable via dwell time switching," *Automatica*, vol. 50, no. 3, pp. 940–945, 2014.
- [16] A. K. Persily, "Ventilation, carbon dioxide and ASHRAE standard 62-1989," *Ashrae J.*, vol. 37, no. 7, pp. 42–44, 1993.
- [17] Z. Huaguang and L. Cai, "Decentralized nonlinear adaptive control of an HVAC system," *IEEE Trans. Syst., Man, Cybern. C, Appl. Rev.*, vol. 32, no. 4, pp. 493–498, Nov. 2002.
- [18] E. Semsar-Kazerouni, M. J. Yazdanpanah, and C. Lucas, "Nonlinear control and disturbance decoupling of HVAC systems using feedback linearization and backstepping with load estimation," *IEEE Trans. Control Syst. Technol.*, vol. 16, no. 5, pp. 918–929, Sep. 2008.
- [19] S. Yuan, B. De Schutter, and S. Baldi, "Adaptive asymptotic tracking control of uncertain time-driven switched linear systems," *IEEE Trans. Autom. Control*, vol. 62, no. 11, pp. 5802–5807, Nov. 2017.
- [20] M. Thiel, D. Schwarzmann, A. M. Annaswamy, M. Schultalbers, and T. Jeansch, "Improved performance for adaptive control of systems with input saturation," in *Proc. Amer. Control Conf.*, Boston, MA, USA, 2016, pp. 6012–6017.
- [21] P. Ioannou and J. Sun, *Robust Adaptive Control*. New York, NY, USA: Dover, 2012.
- [22] W. Sun, Z. Zhao, and H. Gao, "Saturated adaptive robust control for active suspension systems," *IEEE Trans. Ind. Electron.*, vol. 60, no. 9, pp. 3889–3896, Sep. 2013.
- [23] C. Wu, J. Zhao, and X.-M. Sun, "Adaptive tracking control for uncertain switched systems under asynchronous switching," *Int. J. Robust Nonlin. Control*, vol. 25, no. 17, pp. 3457–3477, 2015.
- [24] Q. Sang and G. Tao, "Adaptive control of piecewise linear systems: The state tracking case," *IEEE Trans. Autom. Control*, vol. 57, no. 2, pp. 522–528, Feb. 2012.
- [25] S. Boyd, L. E. Ghaoui, E. Feron, and V. Balakrishnan, *Linear Matrix Inequalities in System and Control Theory*. Philadelphia, PA, USA: SIAM, 1994.
- [26] M.-L. Chiang and L.-C. Fu, "Adaptive control of switched systems with application to HVAC system," in *Proc. 16th IEEE Int. Conf. Control Appl.*, Singapore, 2007, pp. 367–372.
- [27] A. Afram and F. Janabi-Sharifi, "Effects of dead-band and set-point settings of on/off controllers on the energy consumption and equipment switching frequency of a residential HVAC system," *J. Process Control*, vol. 47, pp. 161–174, Nov. 2016.